

Electronic Supplementary Material (ESI)

### **Supporting Information**

Metal-organic framework derived nanoporous carbons with highly selective adsorption and separation of Xenon

Youjin Gong, Yuanming Tang, Zhenghao Mao, Xiaonan Wu, Qiang Liu, Sheng Hu\* Shunshun Xiong\* and Xiaolin Wang

Institute of Nuclear Physics and Chemistry, China Academy of Engineering Physics, Mianyang, Sichuan, 621900, P. R. China. E-mail: [ssxiong@caep.cn](mailto:ssxiong@caep.cn), [husheng205@caep.cn](mailto:husheng205@caep.cn)

## 1. PXRD Analysis

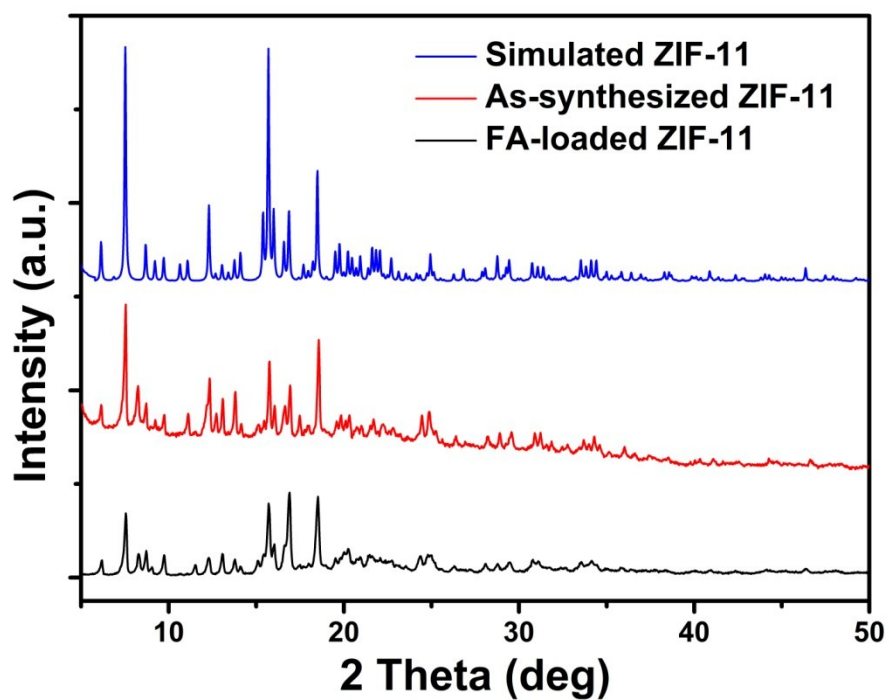


Figure S1. PXRD pattern of ZIF-11 (FA-loaded ZIF-11 is ZIF-11-FA-2 composite)

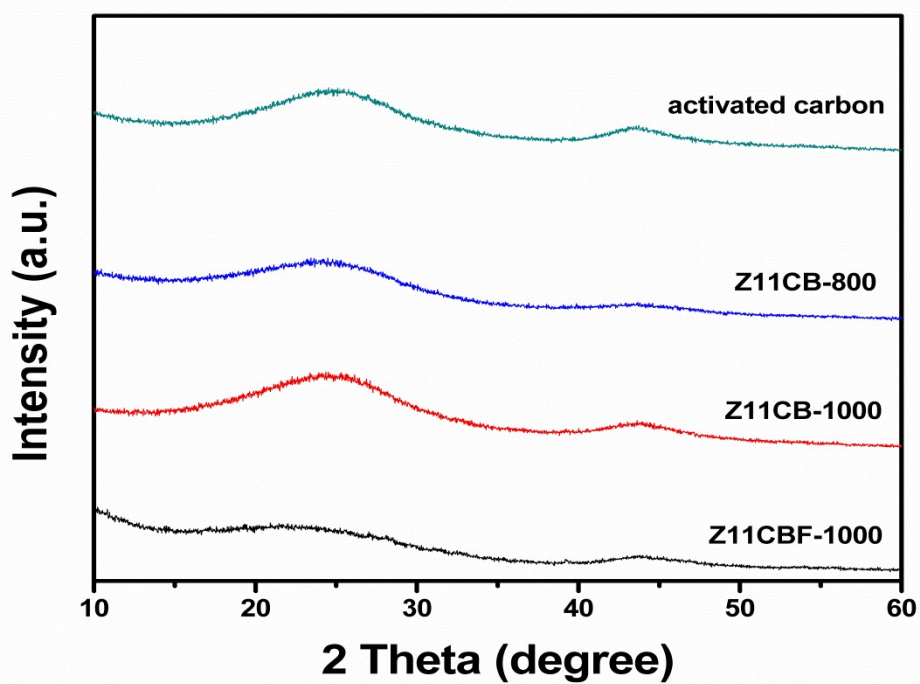
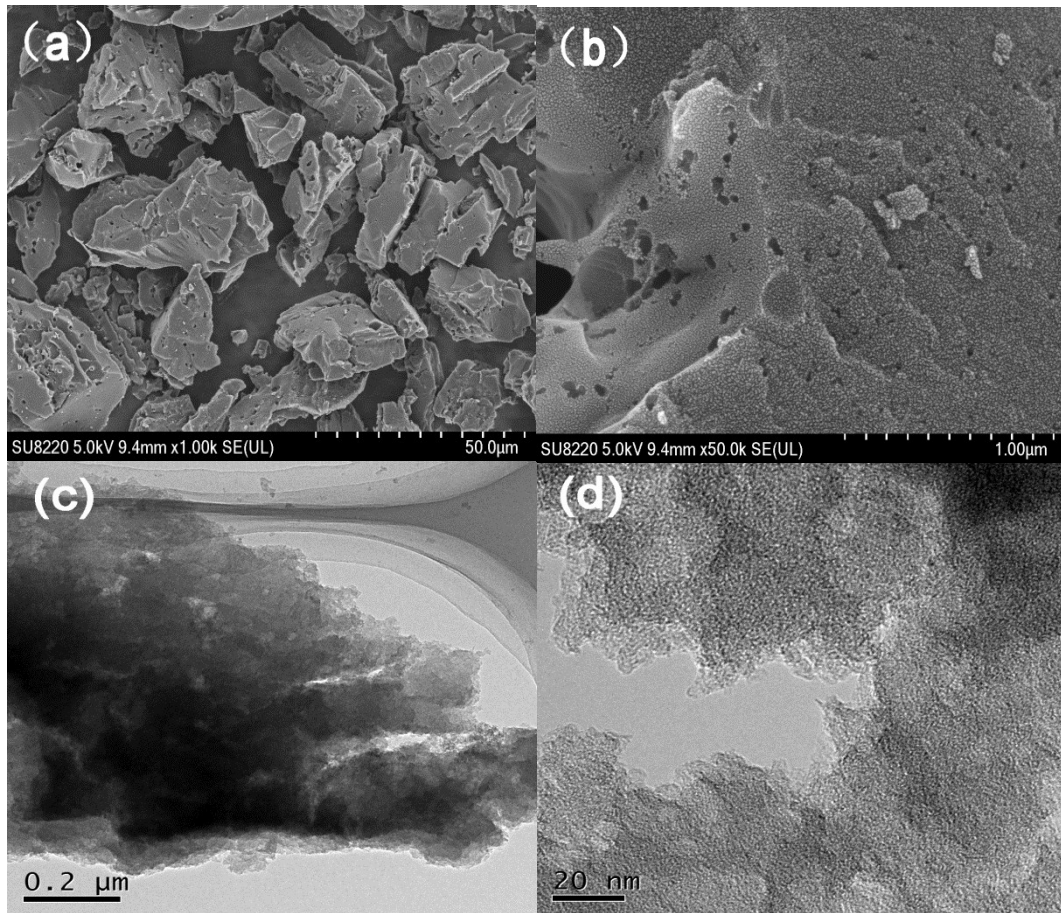
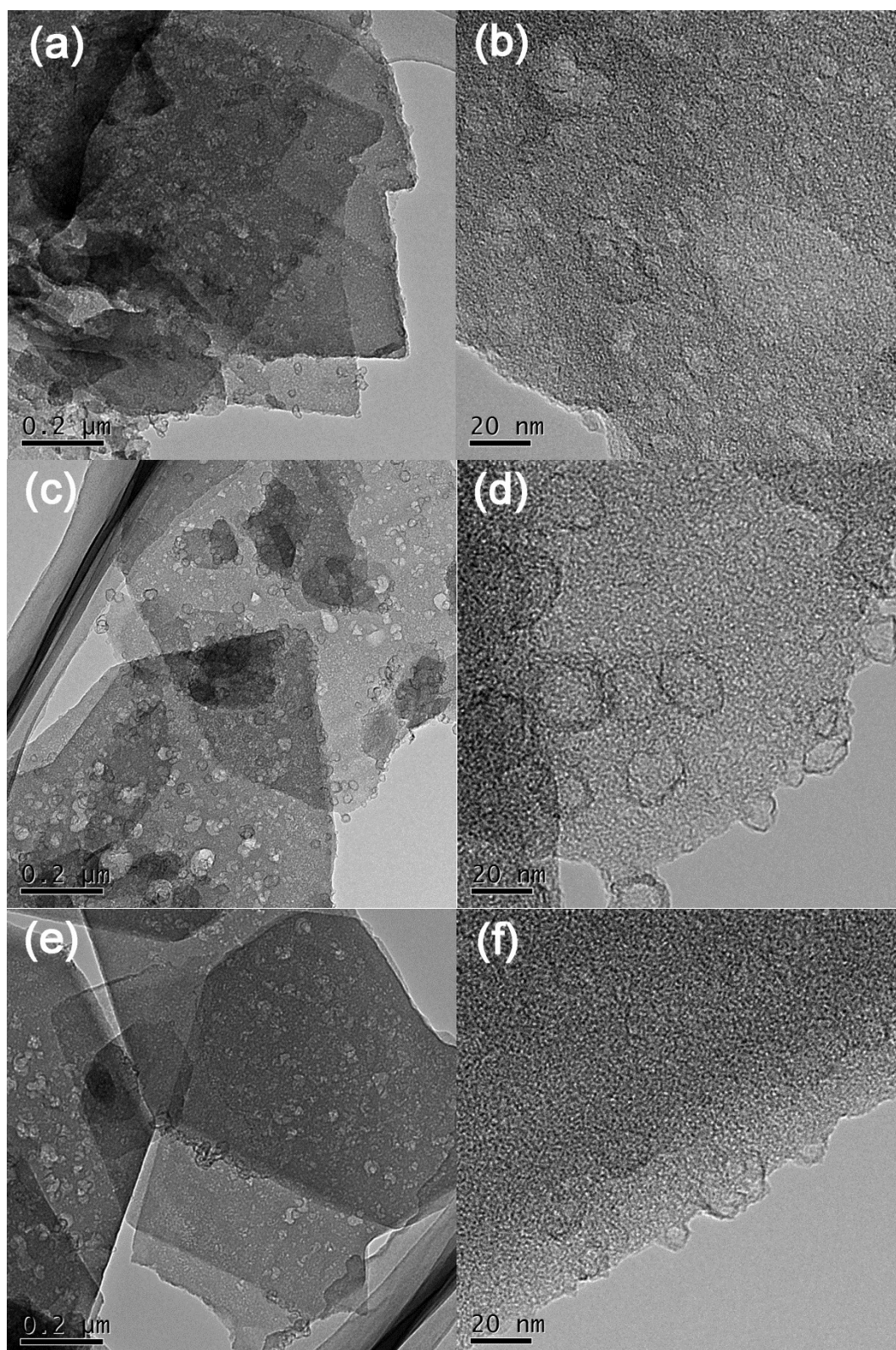


Figure S2. PXRD pattern of Z11CB-800, Z11CB-1000, Z11CBF-1000 and the activated carbon

## 2. SEM and TEM images



**Figure S3.** SEM (a, b) and TEM (c, d) images of the activated carbon



**Figure S4.** TEM images of Z11CBF-1000-2 (a, b), Z11CB-1000 (c, d) and Z11CB-800(e, f)

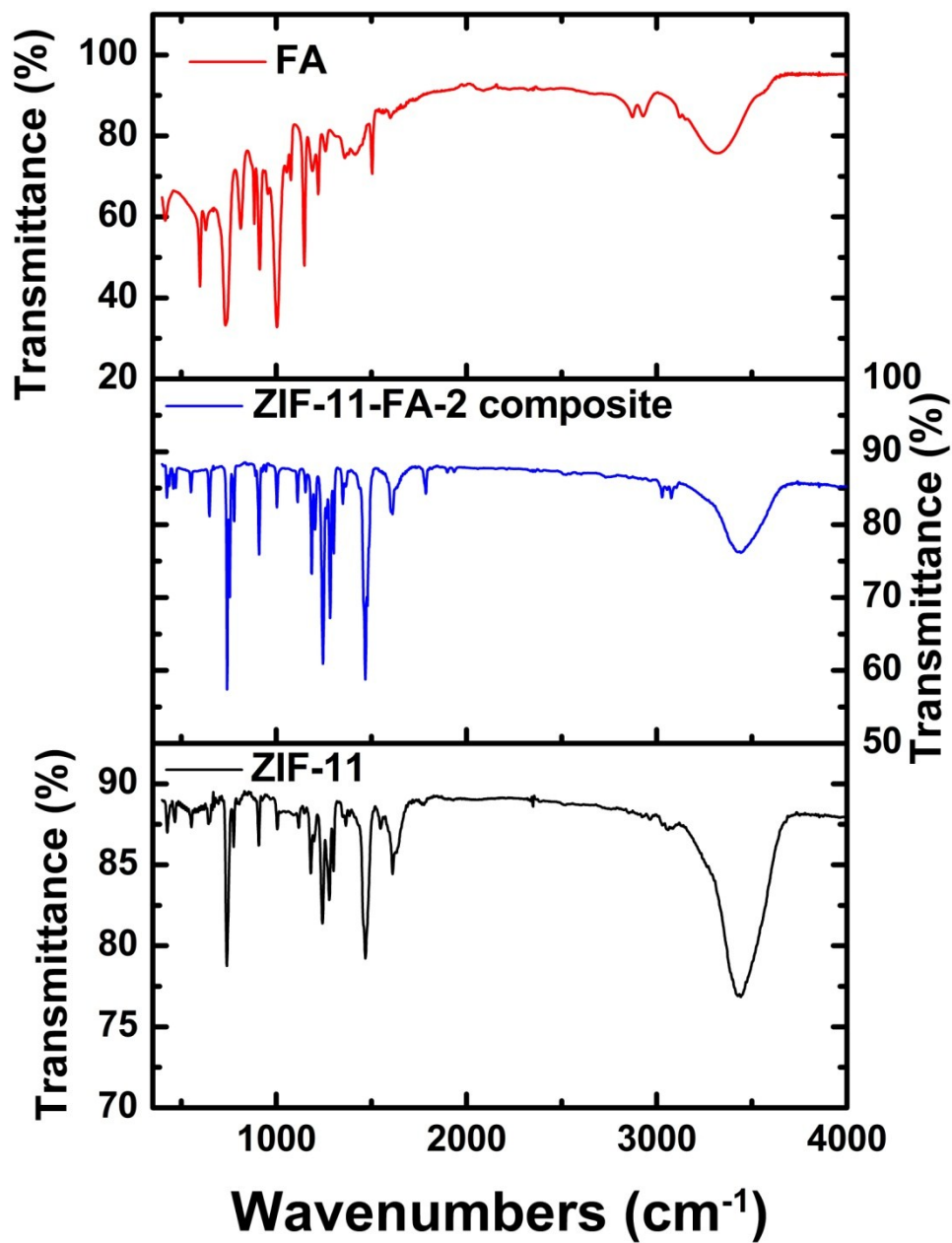


Figure S5. FT-IR curves for FA, ZIF-11 and ZIF-11-FA-2 composite.

### 3. Raman Spectra Analysis

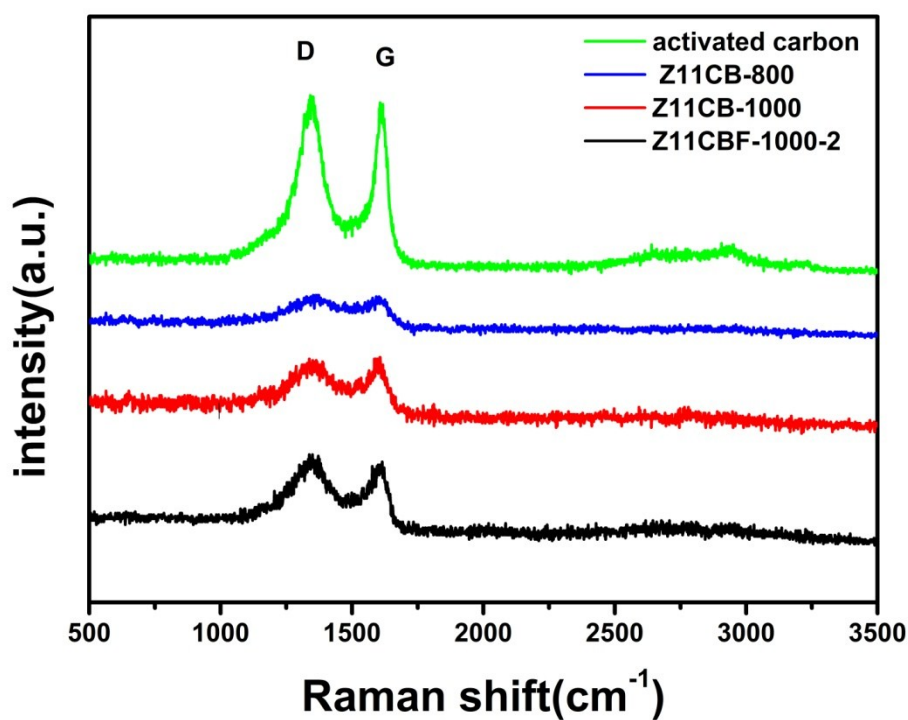


Figure S6. Raman Spectra of Z11CBF-1000-2, Z11CB-1000, Z11CB-800 and the activated carbon

#### 4. XPS Analysis

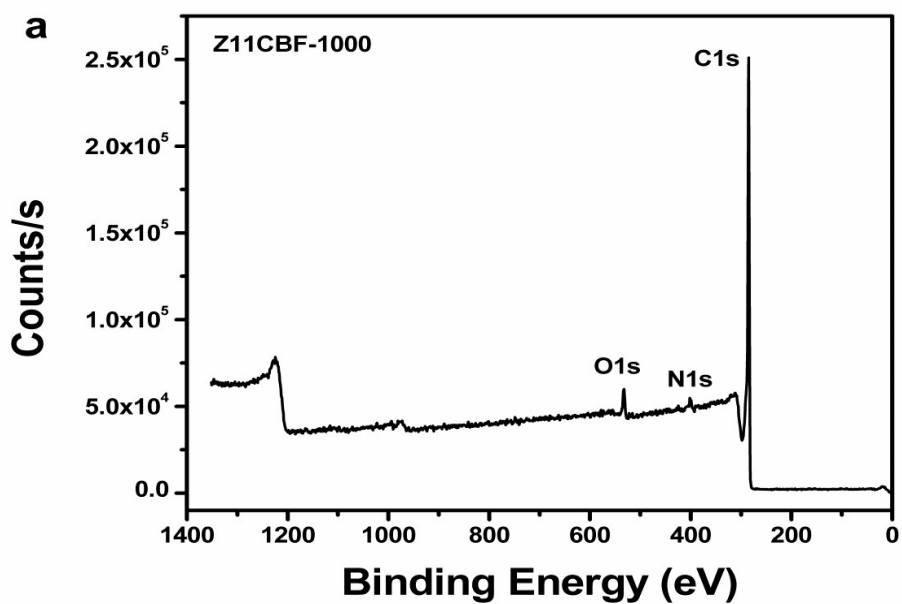


Figure S7. XPS spectra of Z11CBF-1000-2

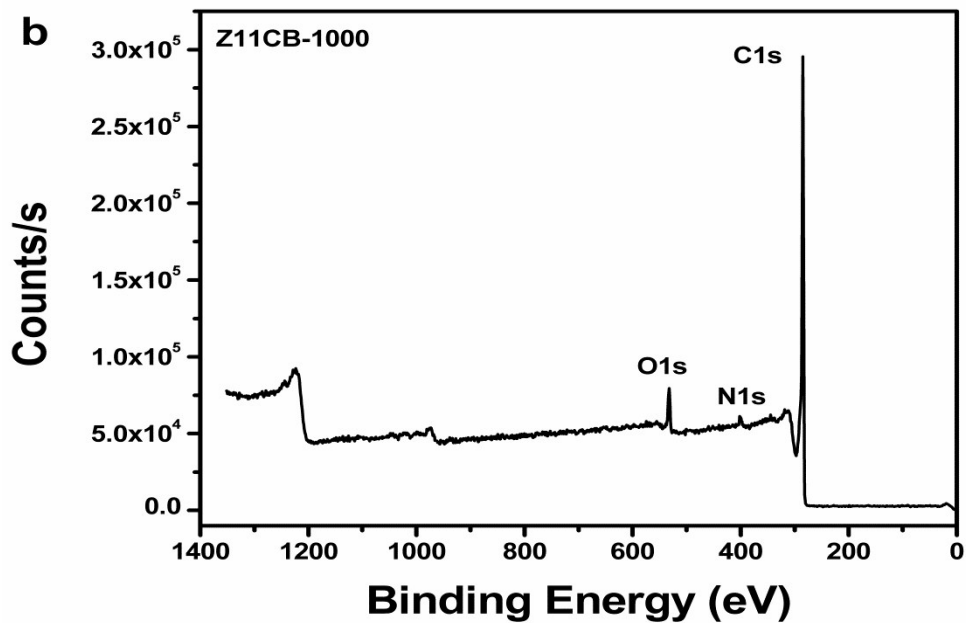


Figure S8. XPS spectra of Z11CB-1000

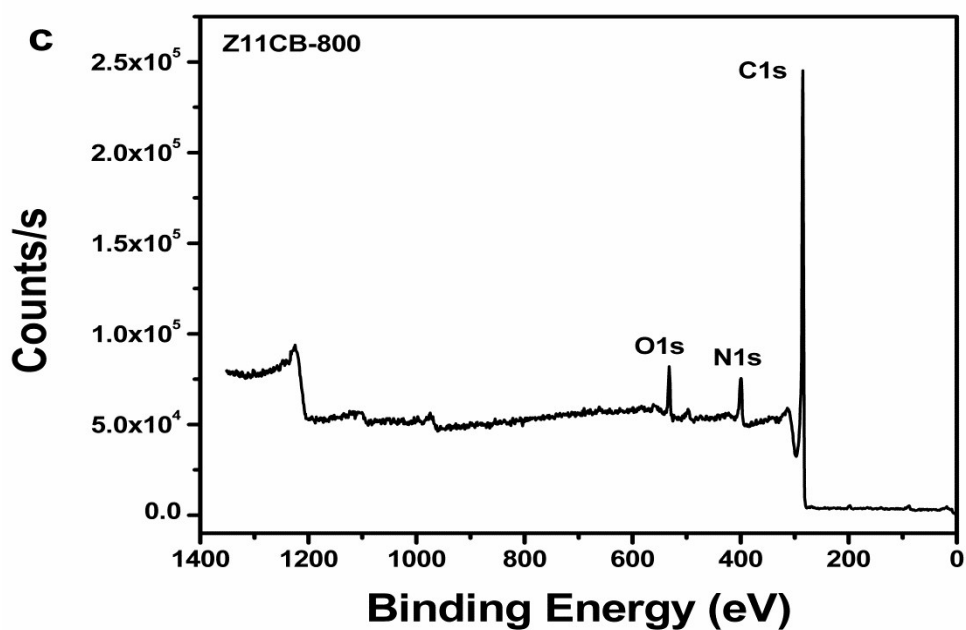
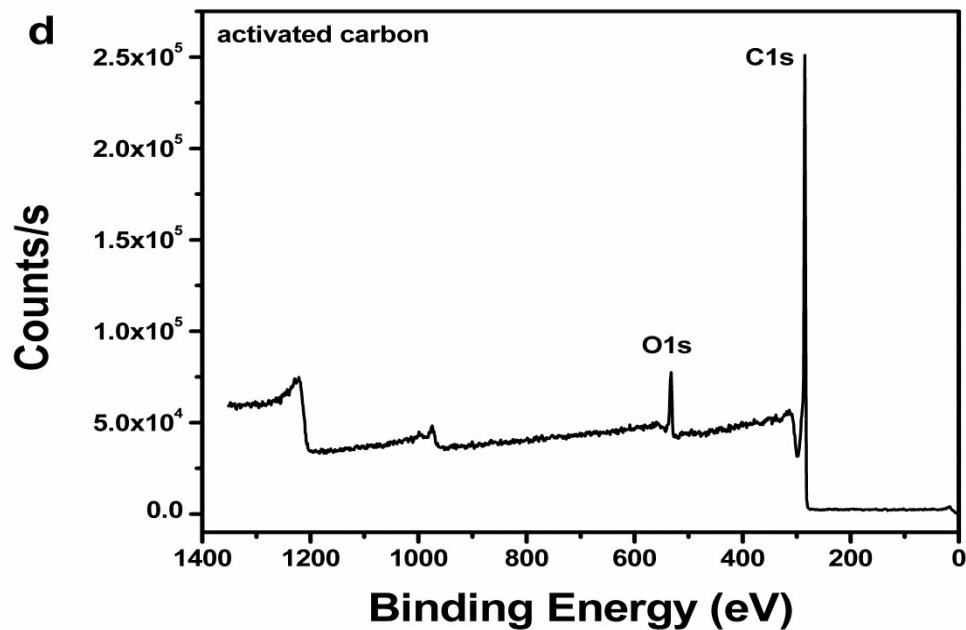


Figure S9. XPS spectra of Z11CB-800



**Figure S10.** XPS spectra of the activated carbon

**Table S1.** Elemental compositions of the porous carbon materials (Z11CBF-1000-2, Z11CB-1100, Z11CB-1000, Z11CB-900, Z11CB-800, Z11CB-700, and AC).

Materials	Elemental composition (at %) determined from XPS		Elemental composition (at %) determined from elemental analysis	
	C	N	C	N
Z11CB-700	-	-	84.83	11.2
Z11CB-800	86.24	8.91	88.77	9.72
Z11CB-900	-	-	90.98	2.44
Z11CB-1000	92.18	2.94	92.54	2.39
Z11CB-1100	-	-	97.76	0.838
Z11CBF-1000-2	94.05	2.7	93.50	2.21
AC	92.65	0.62	92.52	0.57

As the carbonization temperature increases, the N content (wt%) in the NPCs decreases obviously.

## 5. Gas Sorption Measurements

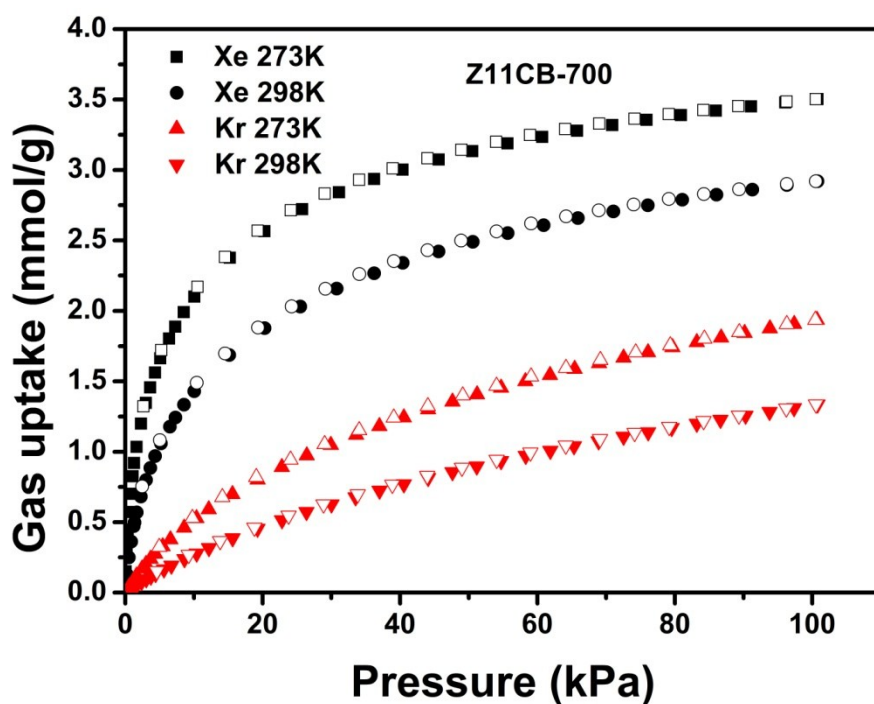


Figure S11. N<sub>2</sub>, Kr and Xe sorption isotherms of the Z11CB-700 at 273K and 298K

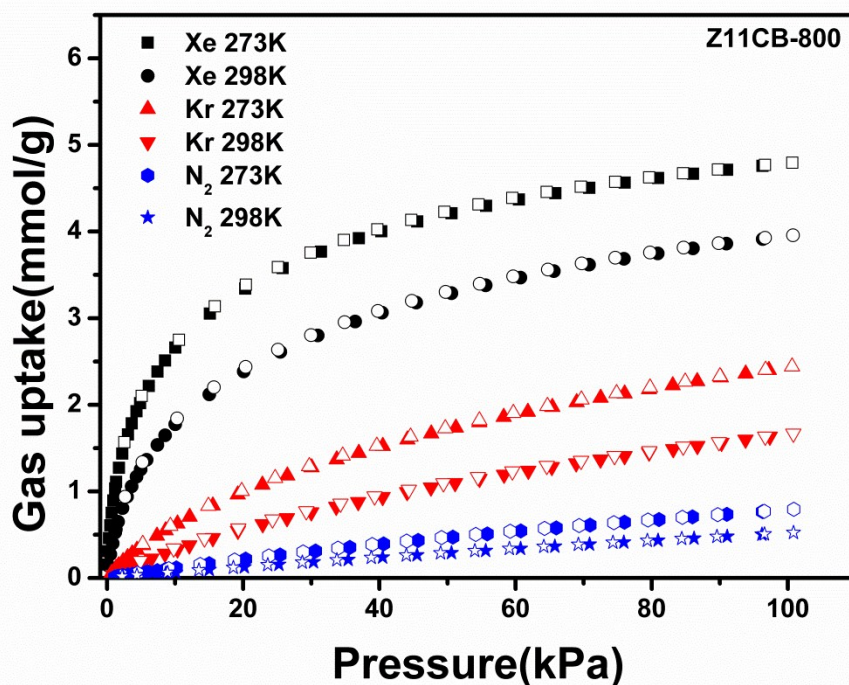


Figure S12. N<sub>2</sub>, Kr and Xe sorption isotherms of the Z11CB-800 at 273K and 298K

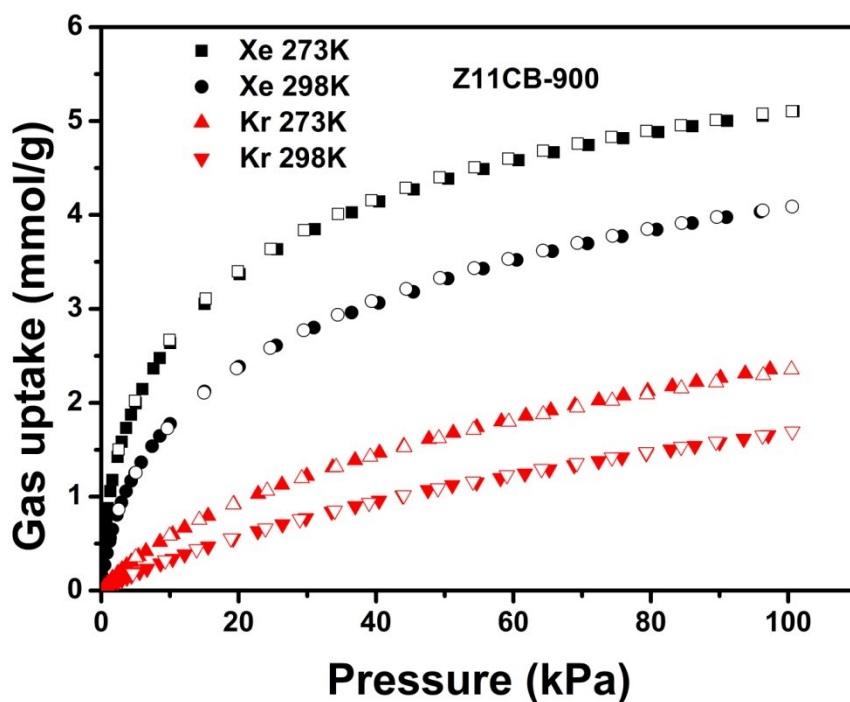


Figure S13.  $N_2$ , Kr and Xe sorption isotherms of the Z11CB-900 at 273K and 298K

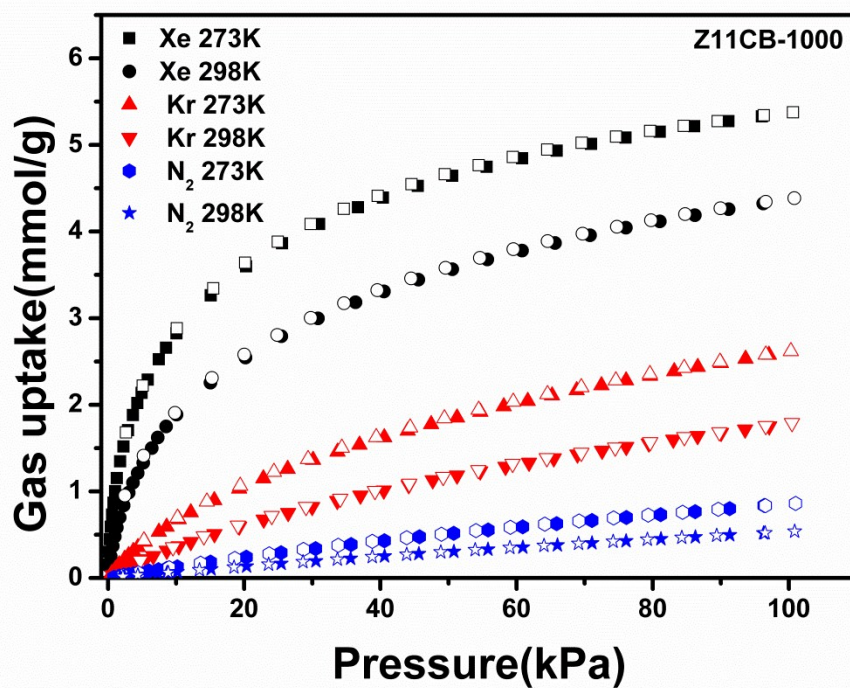


Figure S14.  $N_2$ , Kr and Xe sorption isotherms of the Z11CB-1000 at 273K and 298K

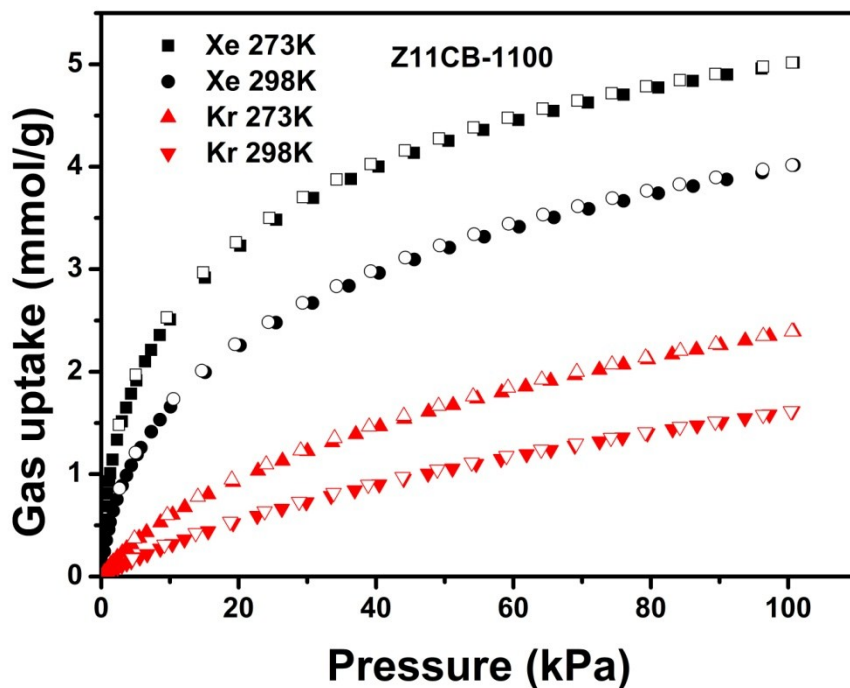


Figure S15. N<sub>2</sub>, Kr and Xe sorption isotherms of the Z11CB-1100 at 273K and 298K

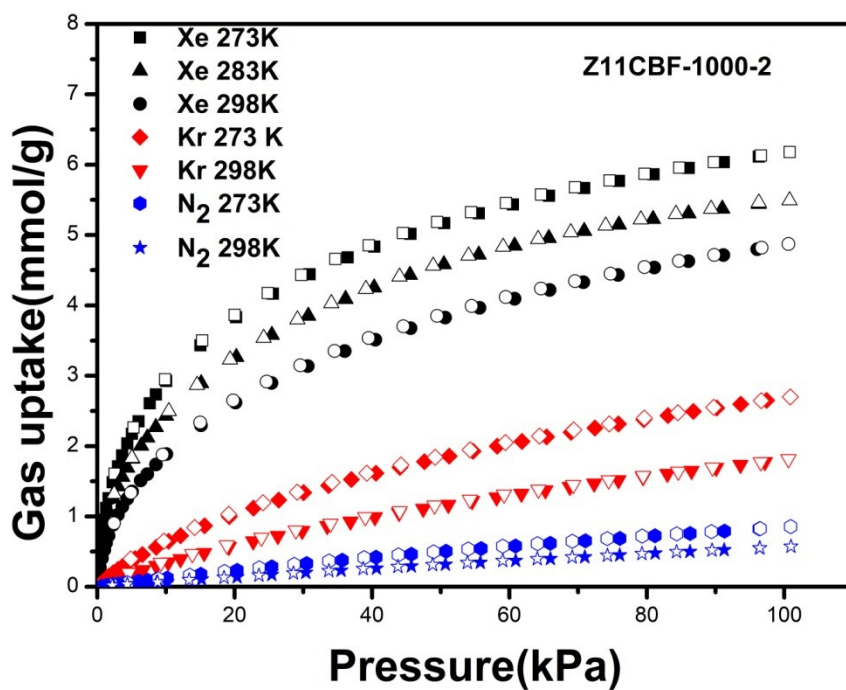


Figure S16. N<sub>2</sub>, Kr and Xe sorption isotherms of the Z11CBF-1000-2.

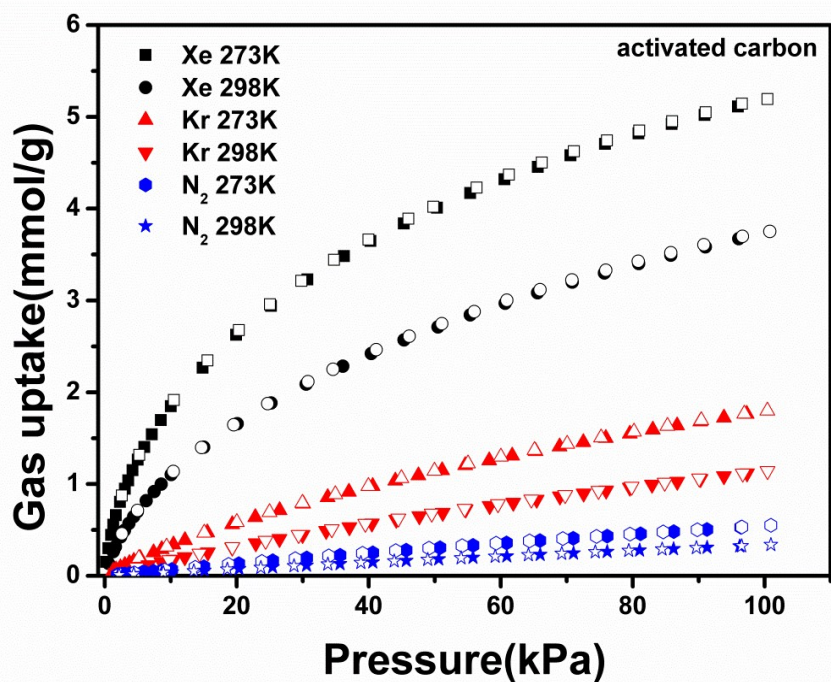


Figure S17. N<sub>2</sub>, Kr and Xe sorption isotherms of AC at 273K and 298K.

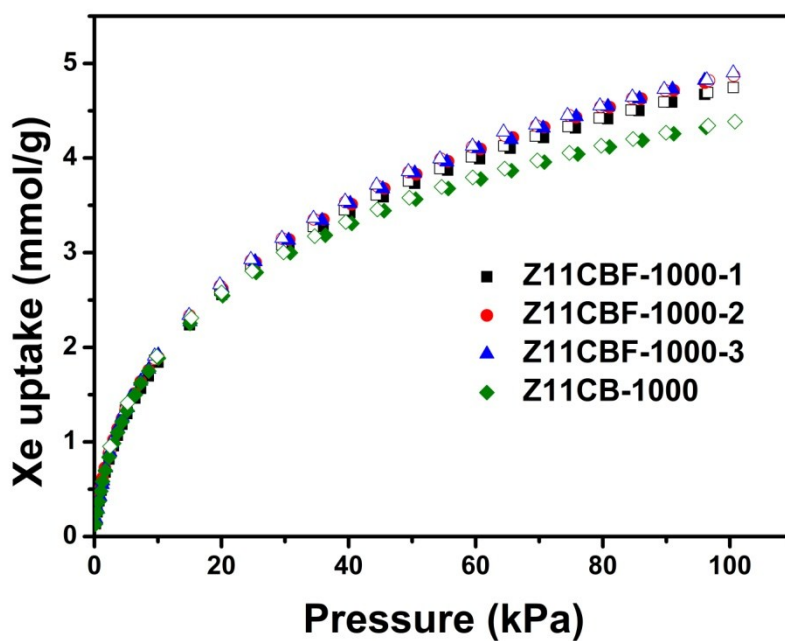
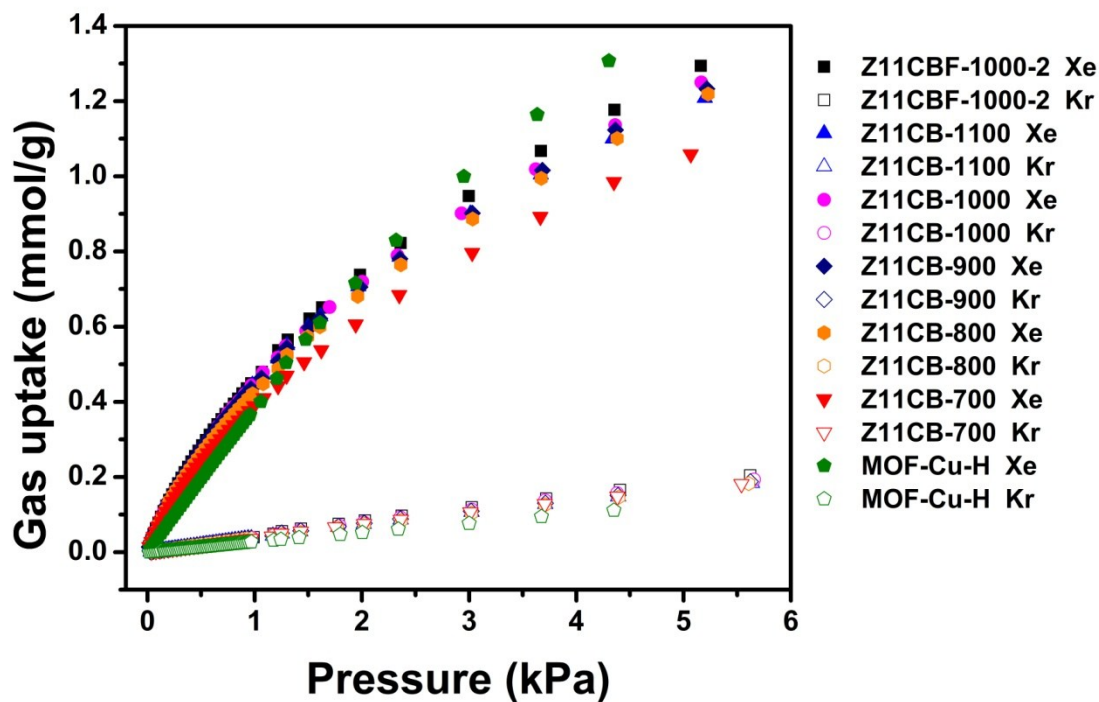
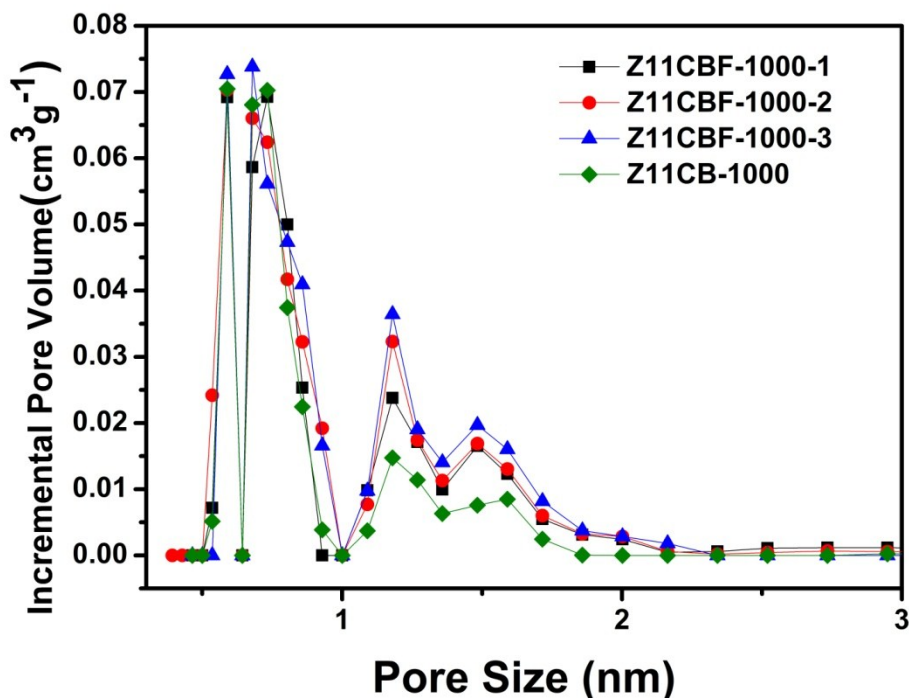


Figure S18. Xe sorption isotherms of Z11CBF-1000-1, Z11CBF-1000-2, Z11CBF-1000-3 and Z11CB-1000 at 298K.



**Figure S19.** Xe and Kr adsorption isotherms for Z11CBF-1000-2, Z11CB-1100, Z11CB-1000, Z11CB-900, Z11CB-800, Z11CB-700, and MOF-Cu-H at low pressure (<6 kPa) at 298K.



**Figure S20.** Pore size distribution curves of Z11CBF-1000-1, Z11CBF-1000-2, Z11CBF-1000-3 and Z11CB-1000 calculated by NLDFT model.

**Table S2.** The calculated Pore size (<10nm) of ZIF-11, Z11CB-700, Z11CB-800, Z11CB-900, Z11CB-1000 Z11CB-1100, Z11CBF-1000-1, Z11CBF-1000-2, Z11CBF-1000-3 and AC based on pore size distribution curves calculated by NLDFIT model.

Materials	Pore size (nm)
ZIF-11	1.2
Z11CB-700	0.59, 1.1, 1.3,
Z11CB-800	0.59, 0.8, 1.2,
Z11CB-900	0.59, 0.68, 1.2, 1.5
Z11CB-1000	0.59, 0.68, 1.2, 1.5
Z11CB-1100	0.68, 0.73, 1.0, 1.2, 7
Z11CBF-1000-1	0.59, 0.73, 1.2, 1.5
Z11CBF-1000-2	0.59, 0.68, 1.2, 1.5
Z11CBF-1000-3	0.59, 0.68, 1.2, 1.5
AC	0.59, 1.2, 1.5, 2.0

## 6. Calculation procedures of isotheric heat of adsorption

The isosteric heat of adsorption ( $Q_{st}$ ) for all the NPCs in this work were calculated by the Clausius-Clapeyron equation based on the adsorption isotherms of Kr and Xe at 273K and 298K.

$$\frac{Q_{st}}{R} = \frac{d(\ln P)}{d(1/T)} \quad (3)$$

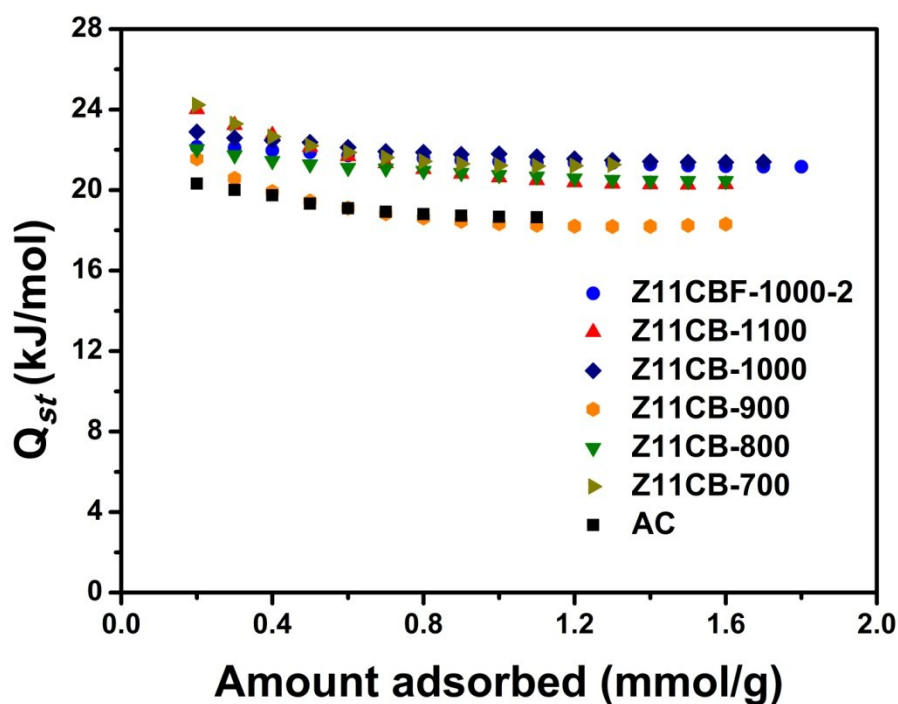


**Figure S21.** The isosteric heats of adsorption ( $Q_{st}$ ) of Xe calculated from adsorption isotherms for, Z11CB-700, Z11CB-800, Z11CB-900, Z11CB-1000, Z11CB-1100, Z11CBF-1000-2 and AC.

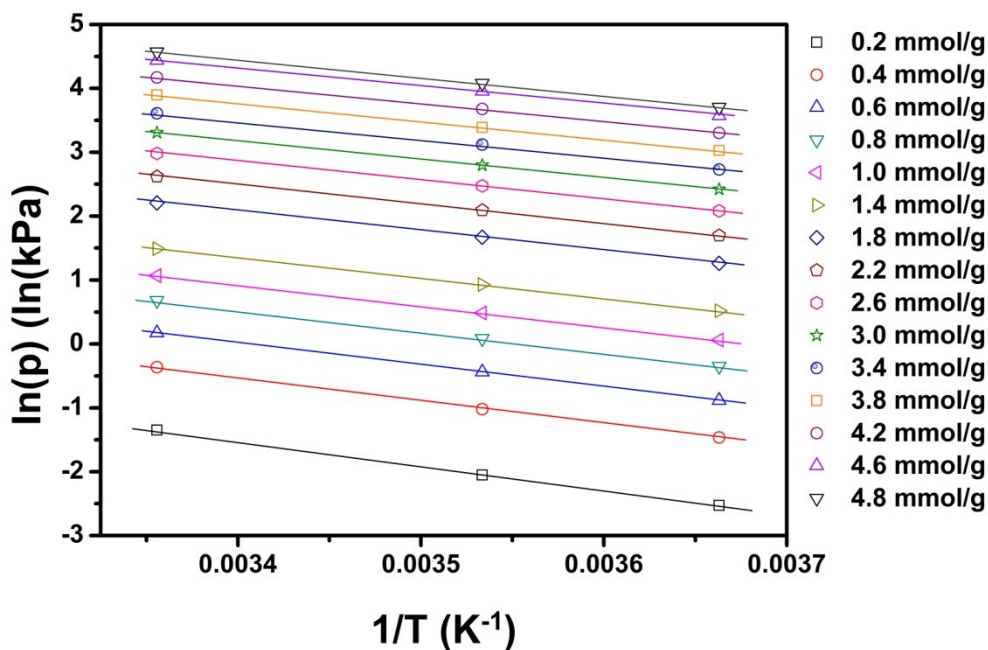


**Figure S22.** Van't Hoff isochore graphs for Xe adsorption on Z11CBF-1000-2 for temperatures 273 K, 283 K and 298 K, as a function of the amount adsorbed ( $n$ ) ranging from 0.2-4.8 mmol/g.

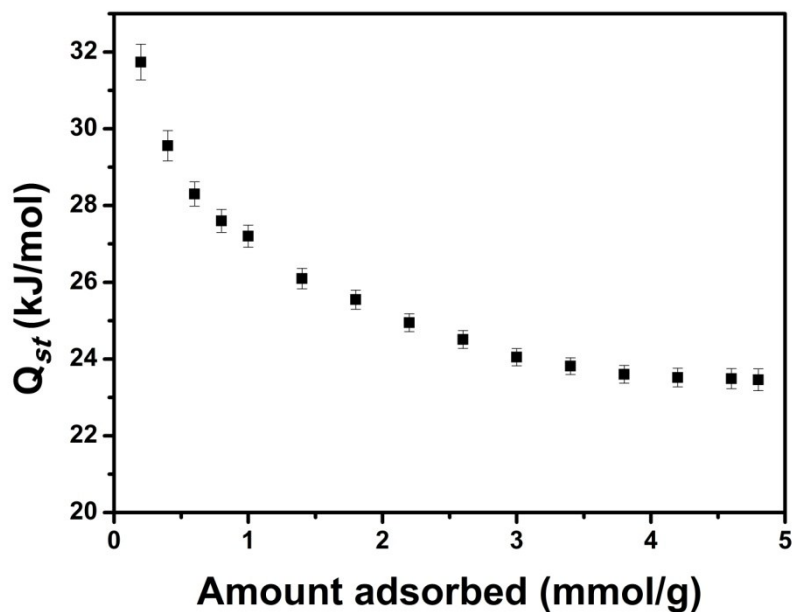


**Figure S23.** Isosteric heat ( $Q_{st}$ / kJ mol<sup>-1</sup>) of adsorption on Z11CBF-1000-2 for Xe as a function of the amount adsorbed (mmol g<sup>-1</sup>) for the temperature range 273-273K.

## 7. Henry's constant fitting

The low range of the adsorption isotherm is nearly linear which corresponds to Henry's law behavior. The Henry's constant for reported materials in this work were obtained from a linear fit to the in low pressure part of the isotherms. The Henry's constants of other reported porous materials were obtained from Thallapally's paper [D. Banerjee, C. M. Simon, A. M. Plonka, R. K. Motkuri, J. Liu, X. Chen, B. Smit, J. B. Parise, M. Haranczyk and P. K. Thallapally, Nat. Commun., 2016, 7, 11831.].

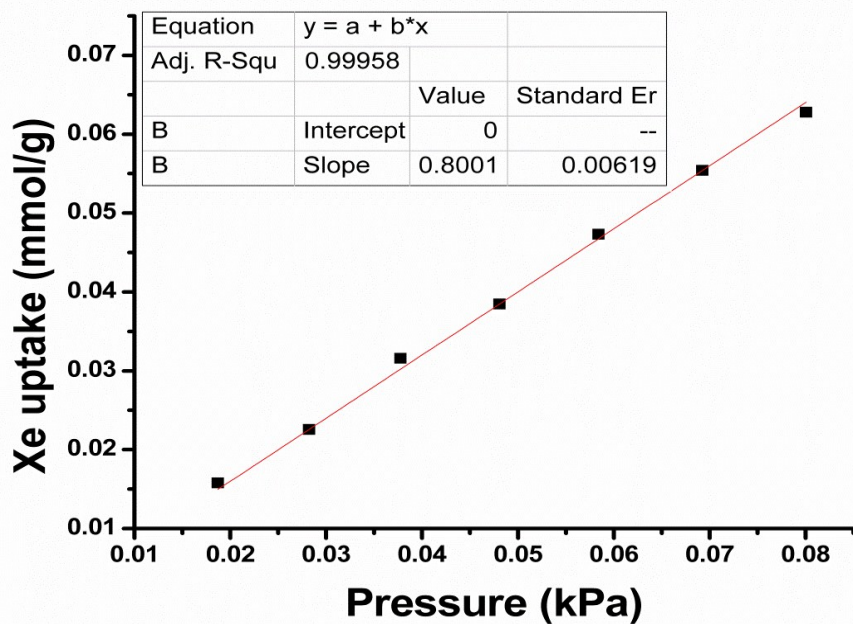


Figure S24. Henry coefficient fitting of Xe adsorption isotherm for Z11CBF-1000-2 at 298K.

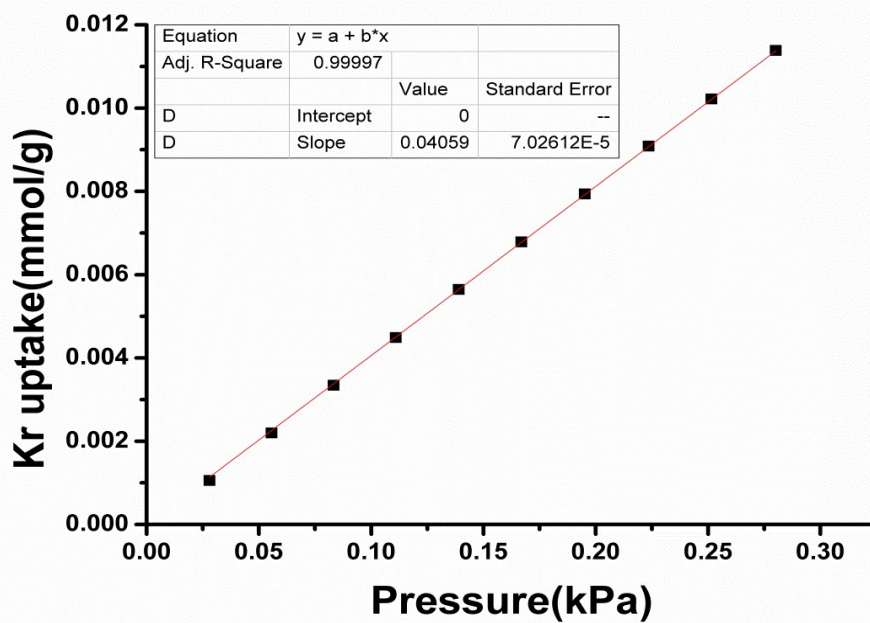


Figure S25. Henry coefficient fitting of Kr adsorption isotherm for Z11CBF-1000-2 at 298K.

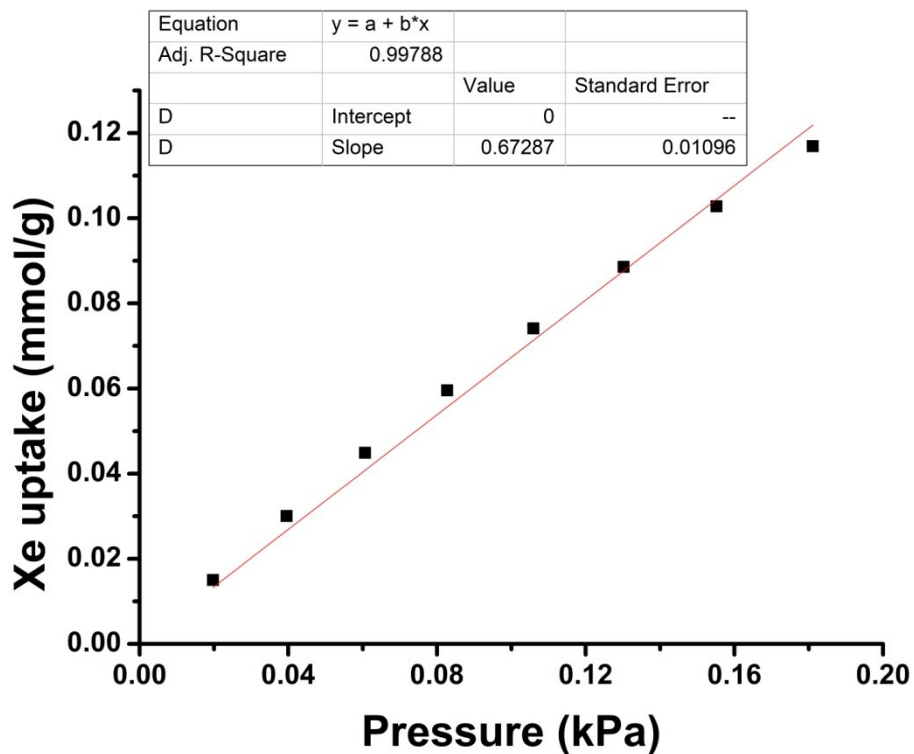


Figure S26. Henry coefficient fitting of Xe adsorption isotherm for Z11CBF-1100 at 298K.

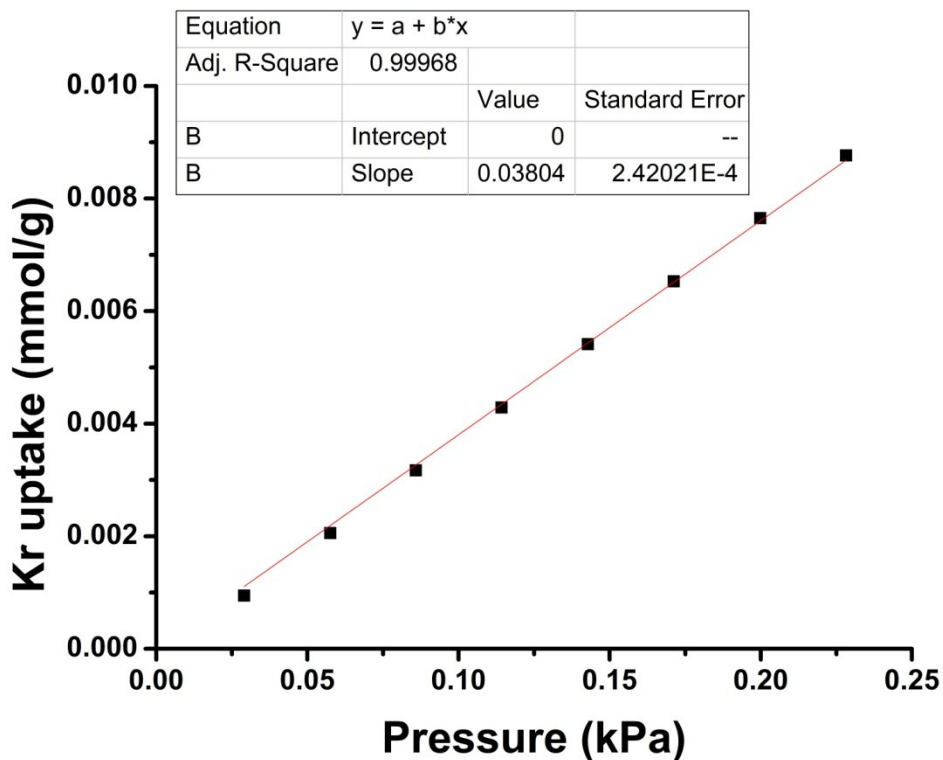


Figure S27. Henry coefficient fitting of Kr adsorption isotherm for Z11CB-1100 at 298K.

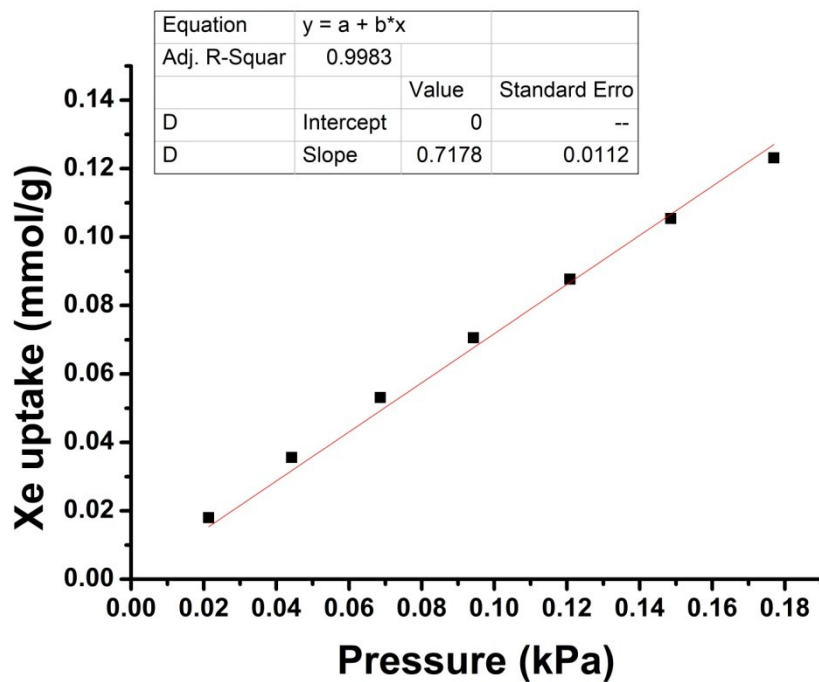


Figure S28. Henry coefficient fitting of Xe adsorption isotherm for Z11CB-1000 at 298K.

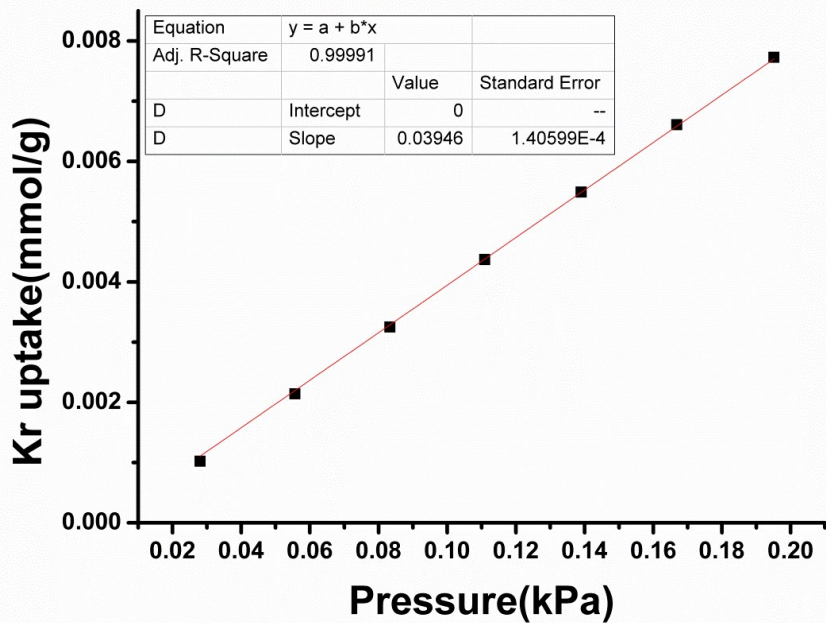
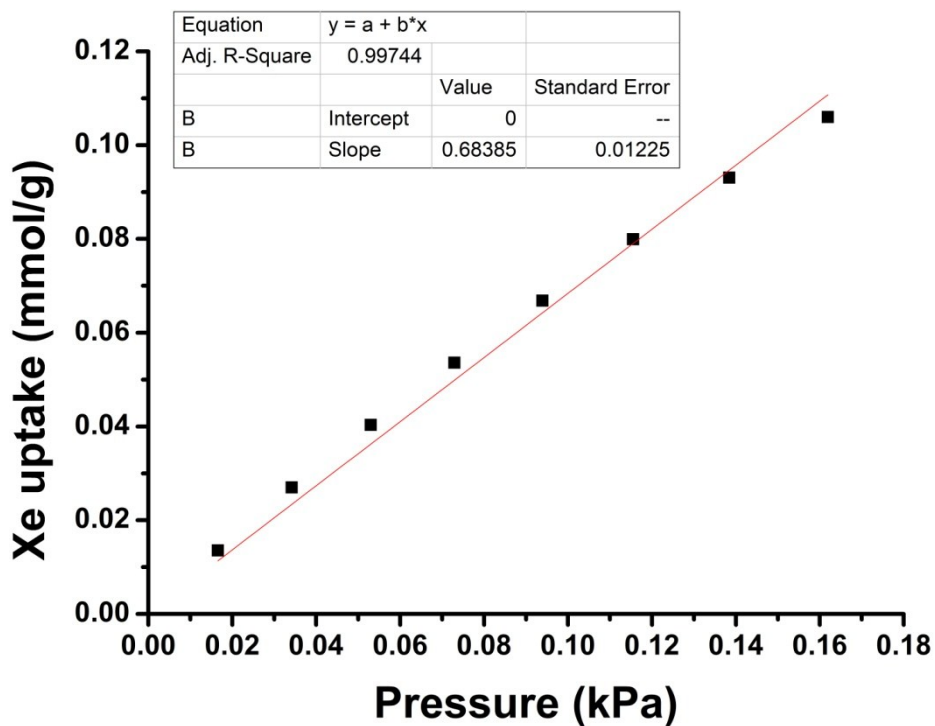
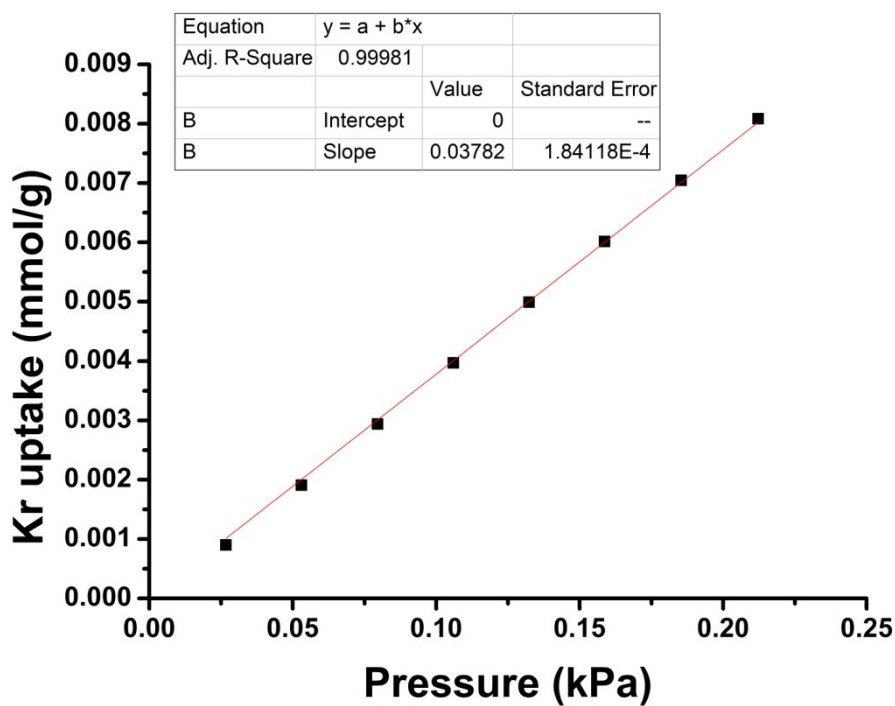


Figure S29. Henry coefficient fitting of Kr adsorption isotherm for Z11CB-1000 at 298K.



**Figure S30.** Henry coefficient fitting of Xe adsorption isotherm for Z11CB-900 at 298K.



**Figure S31.** Henry coefficient fitting of Kr adsorption isotherm for Z11CB-900 at 298K.

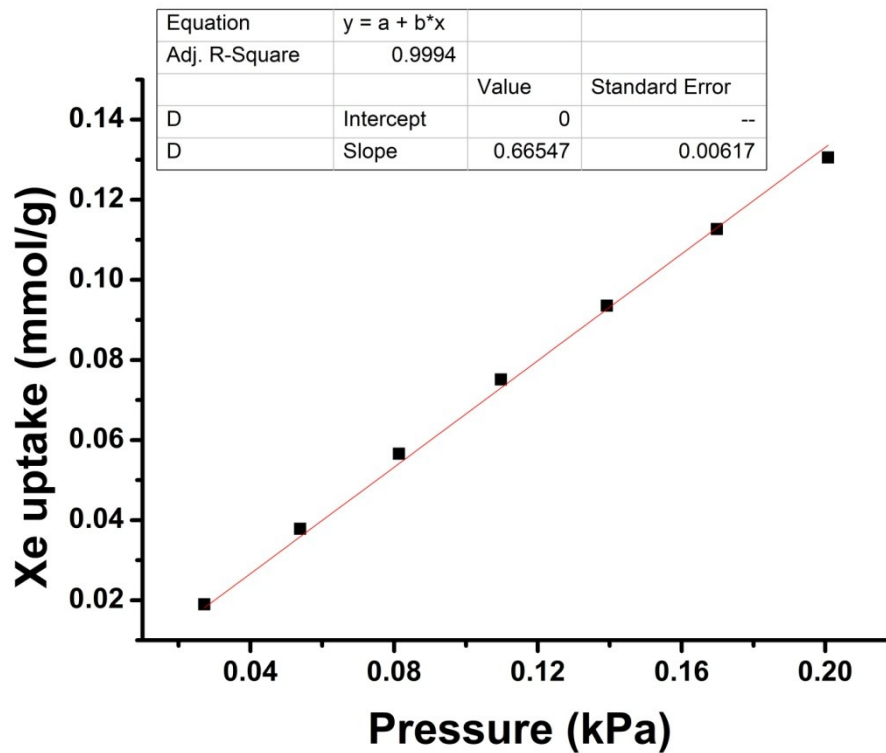


**Figure S32.** Henry coefficient fitting of Xe adsorption isotherm for Z11CB-800 at 298K.

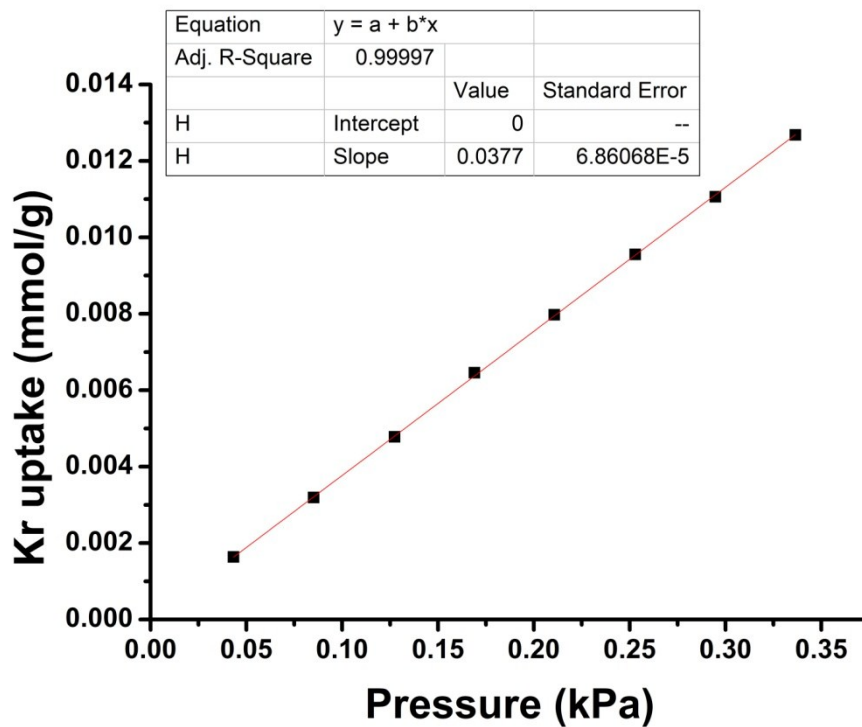


**Figure S33.** Henry coefficient fitting of Kr adsorption isotherm for Z11CB-800 at 298K.

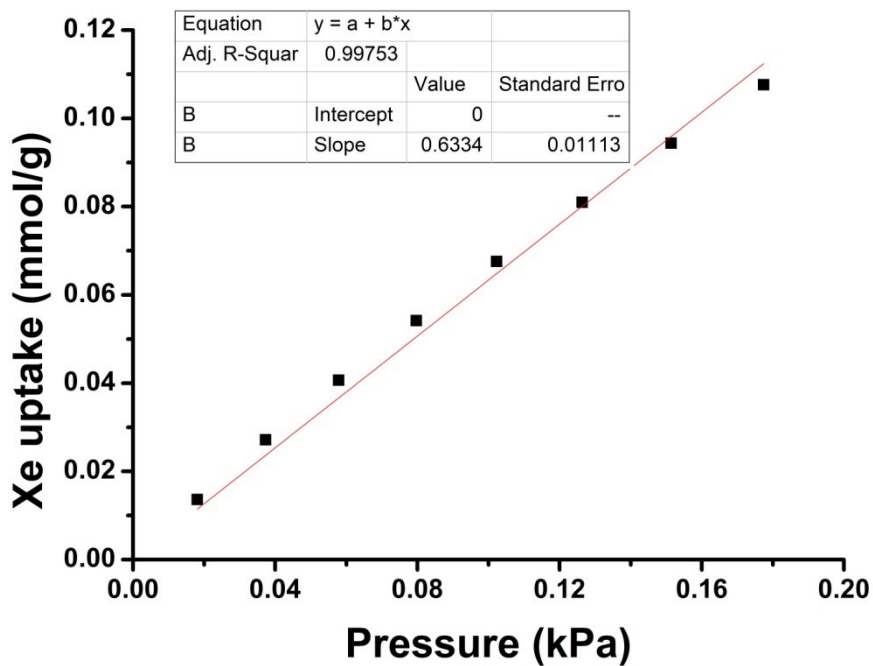


Figure S34. Henry coefficient fitting of Xe adsorption isotherm for Z11CB-700 at 298K.

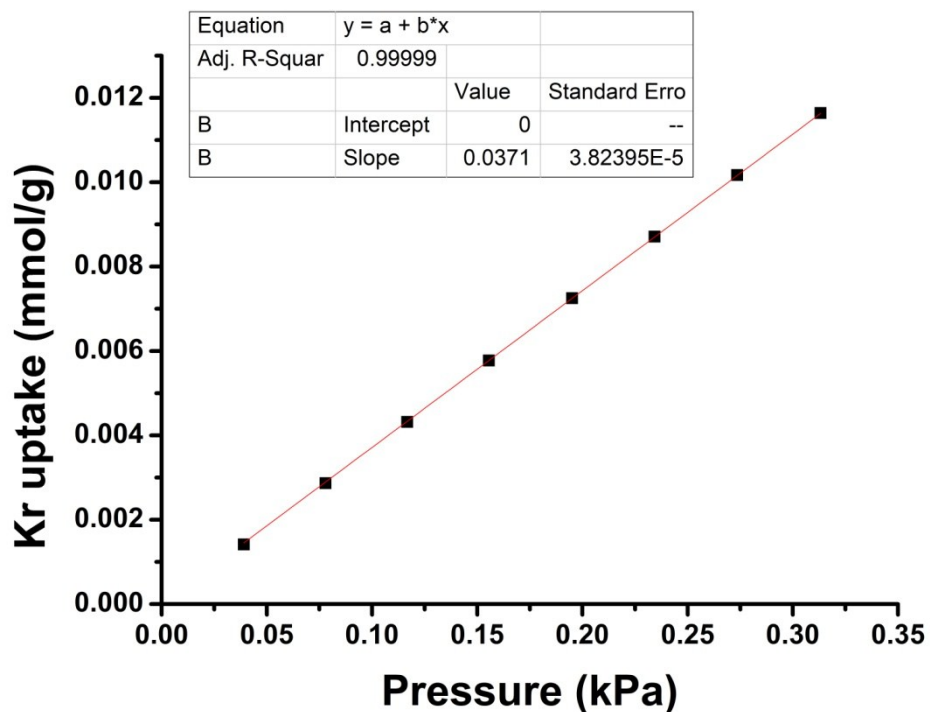
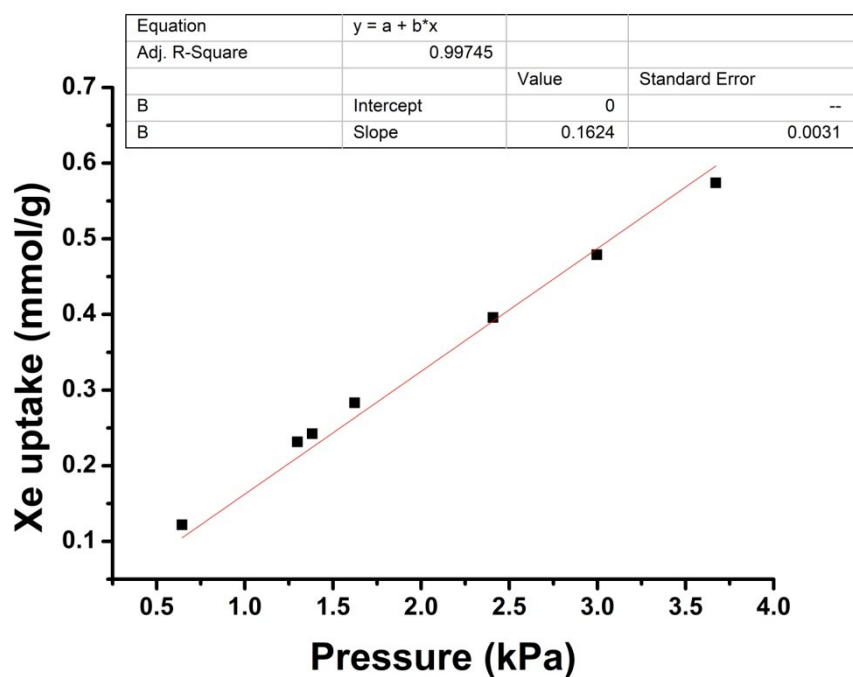
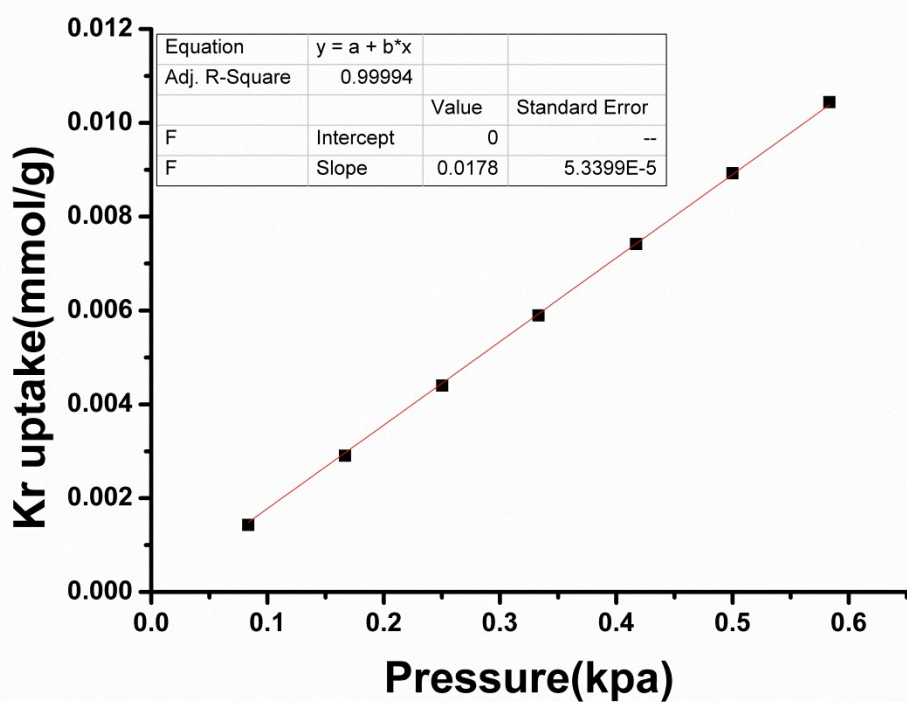


Figure S35. Henry coefficient fitting of Kr adsorption isotherm for Z11CB-700 at 298K.



**Figure S36.** Henry coefficient fitting of Xe adsorption isotherm for the activated carbon at 298K.



**Figure S37.** Henry coefficient fitting of Kr adsorption isotherm for the activated carbon at 298K.

## 8. IAST Selectivity Analysis

### Ideal Adsorption Solution Theory (IAST)

Ideal Adsorbed Solution Theory (IAST) based on pure component isotherms has been demonstrated to be precise in prediction of selectivity of two components gas mixture at low pressure (0-1bar). Herein, IAST of Myers and Prausnitz<sup>1,2</sup> along with the single component adsorption isotherm fittings were used to determine the molar loadings in the mixture for specified partial pressures in bulk phases. The selectivity can be calculated according to the equation:

$$S_{A/B} = \frac{X_A/X_B}{Y_A/Y_B} \quad (1)$$

Where  $X_A$  and  $X_B$  are the mole fractions of the gases A and B in the adsorbed phase and  $Y_A$  and  $Y_B$  are the mole fractions of the gases A and B in the bulk phase.

### Reference

- [1] I. A. L. Myers and J. M. Prausnitz, *AIChE J.*, 1965, 11, 121-130.  
[2] A. L. Myers, *Adsorption*, 2003, 9, 9-16.

### Dual-site Langmuir- Freundlich Fitting of Pure Component Isotherms

On the basis of the Dual site Langmuir-Freundlich (DSLFF) model: (2)

$$N = N_1^{\max} \times \frac{b_1 p^{1/n_1}}{1 + b_1 p^{1/n_1}} + N_2^{\max} \times \frac{b_2 p^{1/n_2}}{1 + b_2 p^{1/n_2}} \quad (2)$$

Where  $p$  (unit: Kpa) is the pressure of the bulk gas at equilibrium with the adsorbed phase,  $N$  (unit: mol/Kg) is the adsorbed amount per mass of adsorbent,  $N_1^{\max}$  and  $N_2^{\max}$  (unit: mol/Kg) are the saturation capacities of sites 1 and 2,  $b_1$  and  $b_2$  (unit: 1/kPa) are the affinity coefficients of sites 1 and 2, and  $n_1$  and  $n_2$  represent the deviations from an ideal homogeneous surface. Here, the single-component Xe and Kr adsorption isotherms have been fit to enable the application of IAST in simulating the performance of porous materials, under a mixed component gas. The fitting parameters of DSLFF equation are listed in Table S1. Adsorption isotherms and gas selectivities calculated by IAST for mixed Xe/Kr (Xe/Kr = 20:80) in the Z11CBF-1000-2, Z11CB-1100, Z11CB-1000, Z11CB-900, Z11CB-800, Z11CB-700, and AC.

**Table S3.** Dual-Langmuir-Freundlich fitting parameters for adsorption isotherms of Xe and Kr in Z11CBF-1000-2, Z11CB-1100, Z11CB-1000, Z11CB-900, Z11CB-800, Z11CB-700, and AC.

adsorbent	Adsorbates	$N_1^{max}$	$b_1$	$n_1$	$N_2^{max}$	$b_2$	$n_2$	$R^2$
Z11CBF-1000-2	Xe	9.46	0.0484	1.54	0.209	0.654	0.562	0.999
	Kr	0.788	0.0373	1.07	4.98	3.61E-3	1.03	0.999
Z11CB-1100	Xe	6.19	0.0354	1.40	1.04	0.284	1.19	0.999
	Kr	4.66	0.00335	1.01	0.624	0.0366	1.02	0.999
Z11CB-1000	Xe	3.12	0.160	1.30	4.22	0.0129	1.15	0.999
	Kr	0.752	0.0342	1.05	5.93	2.86E-3	1.01	0.999
Z11CB-900	Xe	0.652	0.374	1.084	5.58	0.0553	1.38	0.999
	Kr	0.350	0.0603	0.976	4.39	4.34E-3	0.977	0.999
Z11CB-800	Xe	0.657	0.364	0.98	5.28	0.0578	1.37	0.999
	Kr	0.963	0.0277	1.04	4.87	2.92E-3	1.03	0.999
Z11CB-700	Xe	3.59	0.0748	1.37	0.468	0.483	0.940	0.999
	Kr	3.13	0.00319	1.0	0.799	0.0301	1.04	0.999
AC	Xe	0.556	0.146	0.855	7.87	0.0145	1.20	0.999
	Kr	0.371	0.0209	0.952	6.42	0.0019	1.02	0.999

## 9. Breakthrough experiments

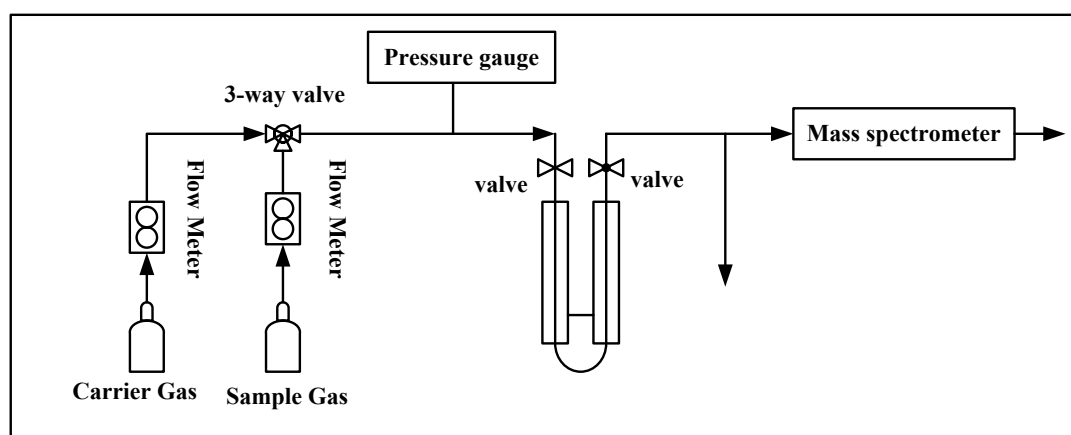


**Figure S38.** Representation of the dynamic breakthrough experiment.

The adsorption capacity was estimated from the breakthrough curves using the following equation:

$$n_{adsi} = FC_i t_i \quad (4)$$

Where  $n_{adsi}$  is the adsorption capacity of the gas  $i$ ,  $F$  is the total molar flow,  $C_i$  is the concentration of the gas  $i$  entering the column and the  $t_i$  is the time corresponding to the gas  $i$ , which is estimated from the breakthrough profile.

The selectivity was then calculated according to the equation:

$$S_{A/B} = \frac{X_A/X_B}{Y_A/Y_B} \quad (5)$$

Where  $X_A$  and  $X_B$  are the mole fractions of the gases A and B in the adsorbed phase and  $Y_A$  and  $Y_B$  are the mole fractions of the gases A and B in the bulk phase.

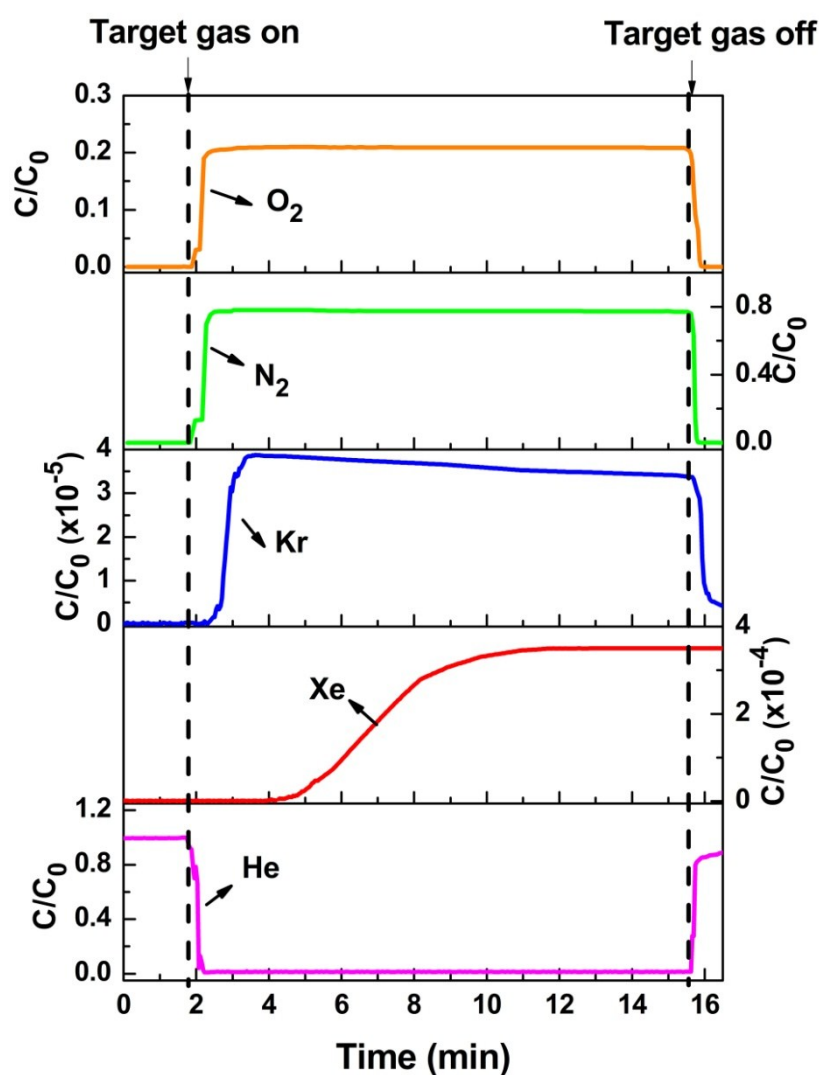


**Figure S39.** Single column breakthrough experiments using AC under low concentrations at 298 K and 1 bar. The column is initially purged with He and then inject with a gas-mixture with 350 p.p.m. Xe and 35 p.p.m. Kr balanced with dry air. The flow rate of He and gas-mixture is 20 ml/min. Xe adsorption capacity of AC was calculated to be 5.6 mmol/kg under this condition.

**Table S4.** Xenon adsorption capacity and Xe/Kr selectivity for reported porous materials at room temperature from gas mixtures at dilute condition

Sorbent	Xe uptake (mmol/kg)	Xe/Kr Selectivity derived from Henry coefficients	Concentration of Xe and Kr
Z11CBF-1000-2	20.6	19.7	350 p.p.m Xe, 35 p.p.m. Kr
AC	5.6	9.1	350 p.p.m Xe, 35 p.p.m. Kr
MOF-Cu-H	13.0	15.8	350 p.p.m Xe, 35 p.p.m. Kr
SBMOF-1	13.2	16.2	400 p.p.m Xe, 40 p.p.m. Kr
CC3	11.0	12.8	400 p.p.m Xe, 40 p.p.m. Kr
Ni-MOF-74	4.8	5.8	400 p.p.m Xe, 40 p.p.m. Kr